Shape coexistence in ^{183}Tl

M. Muikku,[1,*] P. T. Greenlees,[1] K. Hauschild,[2] K. Helariutta,[1,†] D. G. Jenkins,[3] P. Jones,[1] R. Julin,[1] S. Juutinen,[1] H. Kankaanpää,[1] N. S. Kelsall,[3] H. Kettunen,[1] P. Kuusiniemi,[1] M. Leino,[1] C. J. Moore,[4] P. Nieminen,[1] C. D. O'Leary,[3] R. D. Page,[4] P. Rahkila,[1] W. Reviol,[5,‡] M. J. Taylor,[4] J. Uusitalo,[1] and R. Wadsworth[3]

[1]*Accelerator Laboratory, Department of Physics, University of Jyväskylä, FIN-40351 Jyväskylä, Finland*
[2]*CEA Saclay, DAPNIA/SPhN, F-91191 Gif-sur-Yvette Cedex, France*
[3]*Department of Physics, University of York, Heslington, York YO1 5DD, United Kingdom*
[4]*Department of Physics, Oliver Lodge Laboratory, University of Liverpool, Liverpool L69 7ZE, United Kingdom*
[5]*Department of Physics, University of Tennessee, Knoxville, Tennessee 37996*

Prompt and delayed γ rays originating from the neutron deficient nucleus ^{183}Tl have been observed using the recoil-decay tagging and recoil gating techniques. The band-head energy of the prolate $\pi i_{13/2}$ yrast band has been determined. The yrast structure has also been confirmed up to the $(33/2^+)$ state. In addition, a candidate for the $(11/2^-)$ level based on the $\pi(h_{11/2})^{-1}$ configuration has been observed.

I. INTRODUCTION

The even-even light mercury and lead nuclei with $A \leq 190$ provide textbook examples of the shape coexistence phenomenon [1]. In both elements the intruding deformed states (prolate) minimize their energies near the neutron mid-shell at $N=103$ [2,3]. The origin of these deformed states in the Hg and Pb nuclei are proton multi-particle-hole excitations across the $Z=82$ shell [4]. Additional stabilization of the deformed shape near the midshell is obtained from the occupation of low-Ω $i_{13/2}$ neutron orbitals.

In odd-mass Tl ($Z=81$) isotopes, $1p$-$2h$ intruder states and shape coexistence were discovered through the observation of low-lying $9/2^-$ isomeric states [5]. The structure of these isomeric states was confirmed later in an in-beam spectroscopy measurement, where a band of high-spin states was observed to be built on the $9/2^-$ isomer in ^{199}Tl. This was suggested to be due to the odd proton occupying the $h_{9/2}$ intruder orbital giving rise to an oblate shape [6]. Indeed, subsequent laser spectroscopic work for neighboring odd-mass Tl isotopes established a negative quadrupole moment for the $9/2^-$ isomeric state consistent with an oblate shape [7]. Later, rotational bands associated with both oblate ($\pi h_{9/2}, \pi i_{13/2}$) and prolate ($\pi h_{9/2}, \pi i_{13/2}, \pi f_{7/2}$) structures have been observed in lighter isotopes, see e.g., Ref. [8]. The band head of the $(1p$-$2h)$ oblate $\pi h_{9/2}$ intruder band has been observed to lie lowest in energy near $N=108$. In contrast, the band head of the prolate intruder band based on the $\pi i_{13/2}$ structure has been predicted to continue to decrease in excitation energy as the neutron number decreases beyond the neutron midshell point. This prolate structure is presumably formed by coupling the odd $i_{13/2}$ proton to the prolate Hg core of the $4p$-$6h$ structure [8].

Recently, a rotational-like yrast cascade was established in ^{183}Tl and associated with the prolate $\pi i_{13/2}$ structure [10]. However, a linking γ-ray transition from the yrast band down to a lower-lying oblate deformed structure was not observed. Thus, the band-head energy of the yrast band remained uncertain [only upper limit estimate for $E(13/2^+)$ is given in Ref. [10]]. In the present work we have carried out a γ-ray spectroscopy study of ^{183}Tl to determine the band-head energy of this band. Prompt and delayed γ rays from ^{183}Tl were resolved from those arising from the dominant background of fission and other reaction products using the recoil-decay tagging (RDT) [11,12] and recoil gating techniques.

II. EXPERIMENTAL DETAILS

The experiment was carried out at the Accelerator Laboratory of the University of Jyväskylä. Excited states of ^{183}Tl were populated via the ^{144}Sm(^{42}Ca,1p2n) fusion evaporation channel. The ^{42}Ca beam was delivered at an energy of 209 MeV by the JYFL cyclotron. The target consisting of a 500 μg/cm^2 self-supporting metallic ^{144}Sm foil of 92.4% enrichment was used for the first 30 h. For the remaining 120 h, the target was changed to two stacked 500 μg/cm^2 foils. Prompt γ rays were detected by the Jurosphere II array consisting of seven TESSA-type [13], five Nordball [14], and 15 Eurogam Phase I [15] Compton suppressed Ge detectors. At the focal plane, three Nordball and two TESSA-type escape-suppressed Ge detectors placed around the Si detector were used to detect delayed γ rays. The total photopeak efficiencies of the arrays for 1.3-MeV γ rays were about 1.7% and 0.8%, respectively.

The gas-filled recoil separator RITU (Recoil Ion Transport Unit) [16] was used to separate fusion-evaporation residues from the unwanted nuclei such as the primary beam and fission products. RITU is a charge and velocity focusing magnetic device, designed for collecting recoiling fusion-evaporation residues with high efficiency. Separated fusion-

———
*Present address: Radiation and Nuclear Safety Authority, P.O. Box 14, 00881 Helsinki, Finland.

†Present address: Laboratory of Radiochemistry, Department of Chemistry, 00014 University of Helsinki, Finland.

‡Present address: Chemistry Department, Washington University, St. Louis, Missouri 63130.

evaporation residues were implanted into a 80 mm(horizontal) $\times 35$ mm(vertical) Si strip detector covering about 70% of the recoil distribution at the focal plane. The Si detector was also used to detect the subsequent α decay of the implanted recoils. Approximately 50% of the α particles emitted by the recoils were detected with full energy. To purify α-decay events, hits of the Si detector by high energy scattered particles were vetoed by using an additional multiwire proportional avalanche counter (MWPAC) installed 110 mm upstream from the Si detector.

Signals from the Si strip detector for the energy, position, and the detection time of the recoils and α particles were recorded, as well as the γ-ray energies and the detection times from the Ge detectors both at the target position and at the focal plane. The data were recorded if an event in the Si detector was observed.

III. RESULTS

Although the total α-decay branch of the $9/2^-$ level in ^{183}Tl is small ($b \sim 1.5\%$ [17], $t_{1/2} = 60$ ms [18]), the RDT analysis was carried out. The 6.343 ($I \approx 84\%$) and 6.378 MeV ($I \approx 16\%$) [18] α particles and a searching time of 180 ms were used in the tagging procedure. Only the α-decay events under the further condition that the MWPAC did not fire simultaneously with the detection of the α particle were accepted. In Fig. 1 the energy spectra of recoil-gated α-tagged delayed (a) and prompt (b) γ rays are shown. The energies of the prompt 160.1, 260.1, 355.0, 439.4, and 514.6 keV peaks as well as their ordering according to coincidence relationships and relative intensities (Table I) are in accordance with the band observed in the recent recoil-mass selected γ-ray spectroscopic measurement [10]. To document the coincidence relationships, a sample of recoil- and γ-ray gated spectra is shown in Fig. 1(c) (160.1 keV gating transition).

The intensity ratio of γ rays observed by the Ge detectors at 134° and 158° to those observed by the 79° and 101° Ge detectors for the known $E2$ transitions in ^{182}Hg and the 160.1 and 439.4 keV transitions in ^{183}Tl were extracted from the recoil-gated spectra. It was not possible to determine the ratios of the other transitions in ^{183}Tl due to the strong overlapping ^{182}Hg γ-ray energy peaks. The ratios for the 160.1 and 439.4 keV transitions are consistent within error bars with those of the ^{182}Hg $E2$ transitions, thus confirming their $E2$ character. Since these transitions form a high-spin yrast band, it is most likely that all band memebers are of $E2$ character. Indeed, the band in ^{183}Tl resembles the rotation-like $E2$ cascades based on an $i_{13/2}$ state reported for the heavier odd-mass isotopes [8]. In agreement with Ref. [10], the 160-keV γ ray is viewed as the lowest-lying member of the yrast cascade. Consequently, the yrast band in ^{183}Tl is populated down to the presumed $13/2^+$ band head unlike in the heavier isotopes.

The delayed γ-ray spectrum observed at the focal plane of RITU [Fig. 1(a)] shows two clear peaks of 277 and 347 keV in addition to the Tl x rays. A recoil-gated γ-γ matrix was constructed to study coincidence relationships between prompt and delayed γ rays. When gating on the strongest
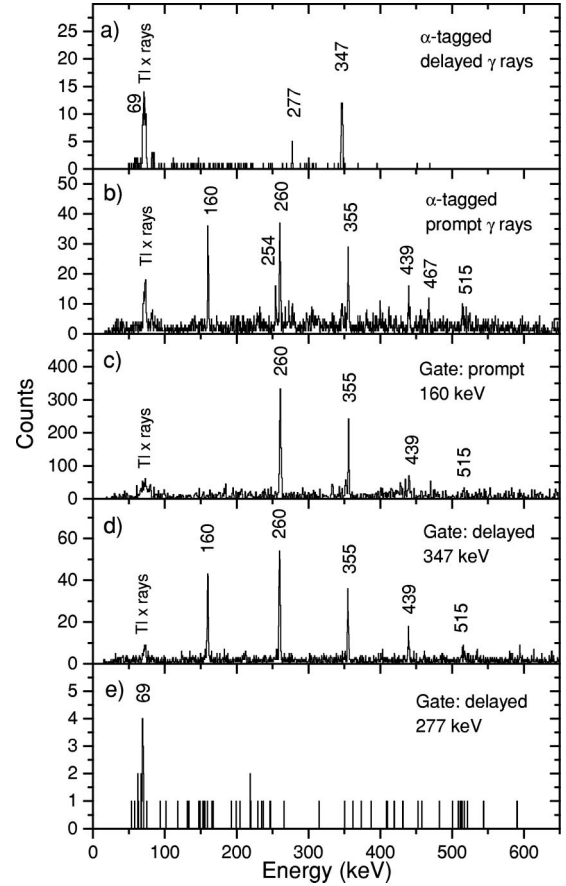

FIG. 1. Energy spectra of (a) delayed and (b) prompt γ-rays generated by gating with recoils and tagging with ^{183}Tl α decays. Energy spectra of prompt γ rays obtained by gating on (c) the prompt 160-keV γ-ray transition and (d) the delayed 347-keV γ-ray transition. (e) Spectrum showing the γ rays observed at the focal plane in coincidence with the 277 keV transition.

delayed transition of 347 keV the energy spectrum of prompt γ rays shown in Fig. 1(d) is obtained. In that spectrum all the above-mentioned transitions of the yrast band are seen. The 347 keV transition is likely to be an $M2$ linking transition from the tentatively assigned $13/2^+$ isomeric state to the $9/2^-$ state, as pointed out later in this paper.

The prompt 160.1, 260.1, 355.0, and 439.4 keV transitions of the yrast band in ^{183}Tl are also seen when gating on the delayed 277 keV transition. This indicates that the 277 keV transition also proceeds in the de-excitation of the presumed ($13/2^+$) isomeric state. In the lowest part of Fig. 1 an energy spectrum of delayed γ rays in coincidence with the 277 keV transition is shown. There is one peak in the spectrum at the energy of 69 keV. This 69-keV γ-ray energy peak is also visible on the low-energy side of the Tl x rays in Fig. 1(a). However, in Fig. 1(e) there is no sign of Tl x rays of 72.9, 70.8, and 82.6 keV although low-energy transitions are usually highly converted. The binding energy of the K electron in Tl nuclei is 85.5 keV and thus, only the L x rays accompanying the conversion electrons are seen in the case of the 69 keV transition. It is not possible to detect such low-energy x rays using the γ-detector array placed at the focal plane. Therefore, no x rays are observed in coincidence

TABLE I. γ-ray transitions in ^{183}Tl.

E_γ (keV)	I_γ (%)[a]	$1 + \alpha_T$	I_i^π	I_f^π	Multipolarity
Prompt γ rays observed in the target position					
160.1(3)	83(9)	1.92	$17/2^+$	$13/2^+$	$E2$
254.1(5)	27(7)				
260.1(3)	100(10)	1.17	$21/2^+$	$17/2^+$	$E2$
355.0(3)	91(10)	1.07	$25/2^+$	$21/2^+$	$E2$
439.4(5)	51(9)	1.04	$29/2^+$	$25/2^+$	$E2$
467.5(5)	49(9)				
514.6(5)	47(9)	1.03	$33/2^+$	$29/2^+$	$E2$
Delayed γ rays observed in the RITU focal plane					
69.3(5)	23(9)	1.24	$13/2^+$	$11/2^-$	$E1$
277.4(5)	10(4)	1.51	$11/2^-$	$9/2^-$	$M1$
346.8(3)	89(10)	1.95	$13/2^+$	$9/2^-$	$M2$

[a]The intensities are normalized to the strongest (260 keV) γ transition.

with 277 keV transition. If we assume $E1$ and $M1$ character for the 69 and 277 keV transitions, respectively, and take into account electron conversion, the intensities of these transitions in the α-tagged spectrum of the delayed γ rays are equal within the errors (see Table I). This fact together with the fast coincidence relationship and energy sum information supports the assumption that the 69 keV and 277 keV transitions are from the $(13/2^+) \rightarrow (11/2^-) \rightarrow (9/2^-)$ cascade.

The half-life of the isomeric state has been determined by fitting a decay curve to the spectrum of the time difference between the implantation of a recoil and the detection of a 347-keV γ ray in the Ge detectors at the RITU focal plane (Fig. 2). The extracted half-life of $t_{1/2} = 1.48(10)$ μs corresponds to a transition strength of $B(M2) = 0.057(10)$ W.u. calculated by taking into account the 347-keV γ-ray transition portion of about 44% of the total de-excitation of the 972 keV level in ^{183}Tl. The transition is hindered by a factor of about 18 compared with the single-particle Weisskopf estimate. In ^{195}Bi and ^{197}At nuclei the $13/2^+ \rightarrow 9/2^-$ transitions have been observed to have hindrance factors of the same order of magnitude (~ 20 and ~ 45, respectively) [19]. The

deduced transition strength strongly supports the assumption that the 347 keV transition in the ^{183}Tl is the $M2$ linking transition from the $(13/2^+)$ yrast band down to a lower-lying oblate deformed $9/2^-$ level. The half-life of $t_{1/2} = 1.3(4)$ μs determined from the time difference between the implantation of a recoil and the detection of a 69-keV γ ray is within errors consistent with the value obtained above by using the 347 keV transition. Assuming $M2$ and $M1$ multipolarities for the 347 and 277 keV transitions the internal K conversion coefficients for these transitions are about 0.7 and 0.4, respectively. The number of observed Tl x rays in the recoil-gated α-tagged spectrum of delayed γ rays are consistent with these coefficients within the error bars.

The deduced level scheme is shown in Fig. 3. The energies of the $1/2^+$, $3/2^+$, and $9/2^-$ levels have been determined in an α-decay study discussed in Ref. [17]. The oblate $13/2^+$ level in ^{183}Tl has not been identified. The 254 and 467 keV transitions are assigned to ^{183}Tl. Due to the limited sta-
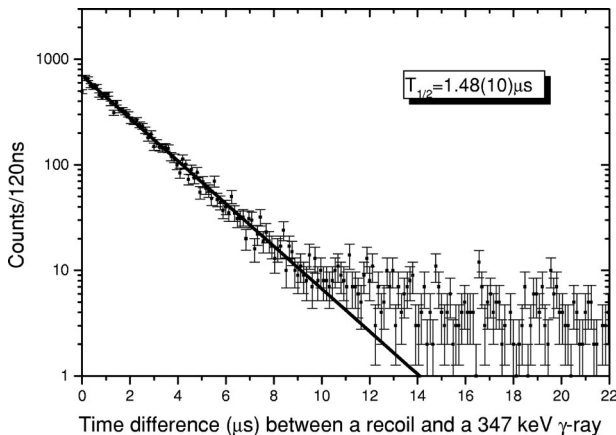

FIG. 2. Spectrum of the time difference between the implantation of a recoil and the detection of a 347-keV γ ray in the Ge detectors at the RITU focal plane.
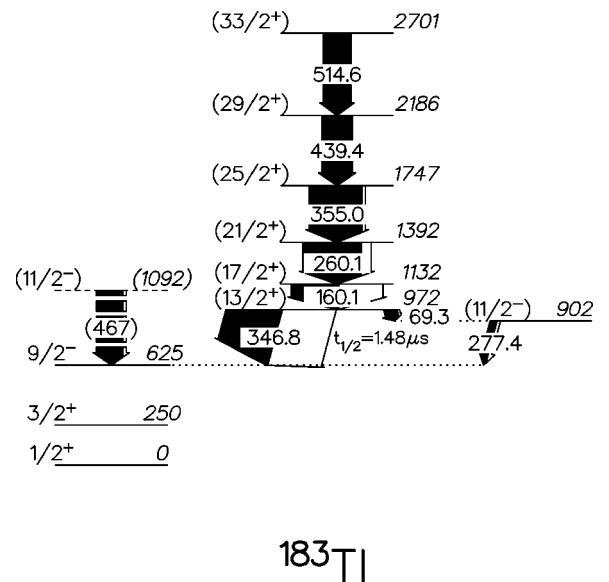

FIG. 3. Level scheme of ^{183}Tl. The energies of the $1/2^+$, $3/2^+$, and $9/2^-$ levels are taken from Ref. [17].
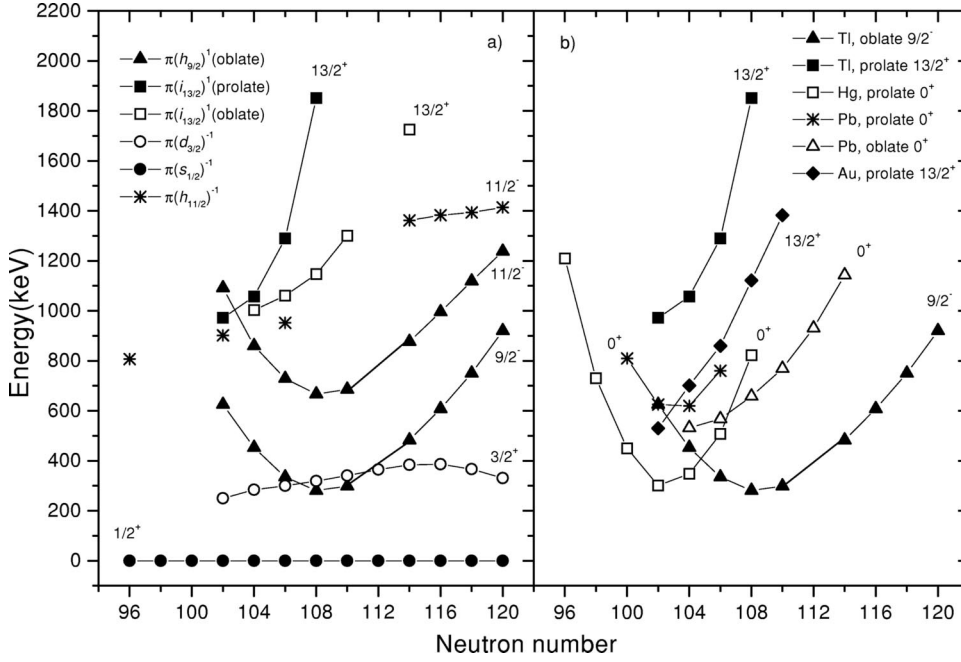
FIG. 4. Comparison of experimentally obtained band-head energies of (a) odd-mass Tl isotopes (b) oblate and prolate deformed bands in Au, Hg, Tl, and Pb isotopes. The data are taken from Refs. [3,8–10,17,20–22,24,26–30] and the present work.

tistics, no γ-γ coincidence information was available to confirm the placements of these transitions. The 467 keV transition is a good candidate for the $11/2^- \rightarrow 9/2^-$ transition seen in the heavier odd-mass Tl isotopes as the strongest transition feeding the oblate isomeric state.

IV. INTERPRETATION

The systematic behavior of observed and extrapolated band-head energies in odd-mass Tl isotopes with $96 \leqslant N \leqslant 120$ is plotted in Fig. 4(a) [8–10,17,20–22,26,27,29]. The two lowest levels of most of these isotopes are the $1/2^+$ (filled circles) and $3/2^+$ (open circles) levels based on the $\pi s_{1/2}$ and $\pi(d_{3/2})^{-1}$ configurations, respectively. Near the neutron number $N=108$ the $9/2^-$ level (filled triangles), the band head of the $(1p$-$2h)$ oblate $\pi h_{9/2}$ intruder band, comes steeply down in energy and it even becomes the second lowest excited level in Tl isotopes with $N=108$ and 110. Both the $9/2^-$ and $11/2^-$ levels of this oblate $\pi h_{9/2}$ band are plotted. The 1092 keV level, tentatively assigned to $11/2^-$ in the present work, has been added to the plot. It follows nicely the systematic trend of the $11/2^-$ members of the oblate band.

The band-head energies of the presumed oblate and prolate $\pi i_{13/2}$ intruder bands are marked with open and filled squares, respectively. The prolate band heads for $^{185-189}$Tl represent extrapolated values based on variable moment of inertia (VMI) fits of the $\pi i_{13/2}$ band and they have been taken from Refs. [8,10]. The band head of ^{183}Tl has been determined in the present work. The unperturbed band head of ^{183}Tl has also been extrapolated using similar VMI fit as in Refs. [8,12]. The value of 975 keV was obtained using the VMI parameters $C=2.98\times10^6$ keV^3 and $\mathfrak{I}=0.0278$ keV^{-1}. The extrapolated band-head energy does not significantly differ from the measured value. Thus, the band heads of the oblate and prolate $\pi i_{13/2}$ bands in ^{183}Tl are not mixed al-

though they are expected to lie close in energy.

In $^{193-201}$Tl the $11/2^-$ level (asterisks) based on the $\pi(h_{11/2})^{-1}$ structure can be seen at the energy of about 1400 keV (see [20] and references therein). This $\pi(h_{11/2})^{-1}$ structure is, supposedly, formed when a $h_{11/2}$ proton hole is weakly coupled to the spherical Pb core. In ^{187}Tl a $11/2^-$ band head tentatively assigned to a weakly prolate-deformed $\pi(h_{11/2})^{-1}$ band has been observed to lie at the energy of 952 keV [8]. In addition, the high-spin isomer in ^{177,179}Tl has been associated with the $\pi(h_{11/2})^{-1}$ configuration rather than the $\pi(h_{9/2})^1$ configuration seen in the heavier isotopes [21,22]. The lowering in the excitation energy of the $11/2^-$ states as a function of neutron number can be explained by assuming that the odd proton is coupled to the prolate Pb core instead of the spherical one. The systematic behavior of the $11/2^-$ levels supports the assumption that the 902 keV level, tentatively assigned in the present work, is the head of the $\pi(h_{11/2})^{-1}$ band.

In Fig. 4(b) the experimentally obtained band-head energies of the oblate $\pi h_{9/2}$ and prolate $\pi i_{13/2}$ bands are plotted together with the energies of the excited 0^+ states in Hg and Pb isotopes. The observed 0^+ states in Pb isotopes based on the oblate structure have been marked with open triangles. The band-head energies of the oblate $\pi h_{9/2}$ bands in the Tl nuclei with $108 \leqslant N \leqslant 114$ are approximately half of the excitation energies of the oblate 0^+ states in the corresponding Pb isotones. This is in accordance with the theoretical predictions [23]. The unperturbed energies of the excited 0^+ states (E_u) in Hg and Pb nuclei assumed to have the prolate shape are marked with open squares and asterisks, respectively. They have been obtained from a fit of the formula $E(I)=AI(I+1)+BI^2(I+1)^2+E_u(0)$ to the known states of energies $E(I)$ assumed to be unmixed members of the prolate band. Near the $N=103$ the prolate intruder bands both in Hg and Pb nuclei reach their minimum energies. As a function of the neutron number, the band-head energy of the prolate $\pi i_{13/2}$ band in Tl isotopes with $N \leqslant 108$ follows the

trend seen in the corresponding Hg isotones. Therefore, if assuming the $4p$-$6h$ configuration for the prolate bands in the Hg nuclei [8,4], the prolate $i_{13/2}$ bands in the Tl nuclei are likely to be based on the $5p$-$6h$ structure. In the Tl nuclei the single $i_{13/2}$ proton seems to act as a spectator without disturbing the prolate structure of the Hg core. Thus, the occupation probability of the $i_{13/2}$ prolate orbits is small in the wave function of the prolate minimum of the core as already noted in Ref. [8,25].

It is not clear whether, unlike in the neighboring Hg and Pb nuclei, the band head of the $\pi i_{13/2}$ prolate band in odd-mass Tl isotopes continues to drop in excitation energy when going towards the more neutron-deficient side. In the odd-mass Au isotopes the $\pi i_{13/2}$ prolate band [filled diamonds in Fig. 4(b)] does not seem to reach the minimum energy above $N=100$ although the calculations [24] predict that the energy of this configuration should lie lowest at $N=102$. As shown in Fig. 4(b), the drop in excitation energy is steeper for the Au nuclei than for the Tl nuclei. In Ref. [8] the prolate states in odd-mass Tl isotopes are predicted to continue to drop in energy when passing the midshell, while the calculations presented in Refs. [25] show a rise in excitation energy at $N=104$. In this respect, it would be of interest to probe the level structure of the ^{181}Tl isotope.

V. SUMMARY

In the present work the band-head energy of the prolate $\pi i_{13/2}$ yrast band in ^{183}Tl has been determined. The yrast sequence has also been confirmed up to the $(33/2^+)$ state using the RDT technique. In addition, a candidate for the $(11/2^-)$ level based on the $\pi(h_{11/2})^{-1}$ configuration has been observed. The obtained results support the assumption that the prolate band is based on a $5p$-$6h$ structure formed by coupling the odd $i_{13/2}$ proton to the prolate $(4p$-$6h)$ Hg core. However, the question whether the band head of the $\pi i_{13/2}$ band in odd-mass Tl isotopes continues to drop in excitation energy beyond the neutron midshell remains open.

[1] J.L. Wood, K. Heyde, W. Nazarewicz, M. Huyse, and P. Van Duppen, Phys. Rep. **215**, 101 (1992).

[2] G.D. Dracoulis, A.E. Stuchbery, A.O. Macchiavelli, C.W. Beausang, J. Burde, M.A. Deplanque, R.M. Diamond, and F.S. Stephens, Phys. Lett. B **208**, 365 (1988).

[3] D.G. Jenkins et al., Phys. Rev. C **62**, 021302(R) (2000).

[4] W. Nazarewicz, Phys. Lett. B **305**, 195 (1993).

[5] R.M. Diamond and F.S. Stephens, Nucl. Phys. **45**, 632 (1963).

[6] J.O. Newton, S.D. Cirilov, F.S. Stephens, and R.M. Diamond, Nucl. Phys. **A148**, 593 (1970).

[7] J.A. Bounds, C.R. Bingham, P. Juncar, H.K. Carter, G.A. Leander, R.L. Mlekodaj, E.H. Spejewski, and W.M. Fairbank, Jr., Phys. Rev. Lett. **55**, 2269 (1985).

[8] G.J. Lane et al., Nucl. Phys. **A586**, 316 (1995).

[9] M.-G. Porquet et al., Phys. Rev. C **44**, 2445 (1991).

[10] W. Reviol et al., Phys. Rev. C **61**, 044310 (2000).

[11] R.S. Simon et al., Z. Phys. A **325**, 197 (1986).

[12] E.S. Paul et al., Phys. Rev. C **51**, 78 (1995).

[13] P.J. Nolan, D.W. Gifford, and P.J. Twin, Nucl. Instrum. Methods Phys. Res. A **236**, 95 (1985).

[14] M. Moszÿnski, J.H. Bjerregard, J.J. Gaardhøje, B. Herskind, P. Knudsen, and G. Sletten, Nucl. Instrum. Methods Phys. Res. A **280**, 73 (1989).

[15] C.W. Beausang et al., Nucl. Instrum. Methods Phys. Res. A **313**, 37 (1992).

[16] M. Leino et al., Nucl. Instrum. Methods Phys. Res. B **99**, 653 (1995).

[17] J.C. Batchelder et al., Eur. Phys. J. A **5**, 49 (1999).

[18] U.J. Schrewe et al., Phys. Lett. **91B**, 46 (1980).

[19] M.B. Smith et al., Eur. Phys. J. A **5**, 43 (1999).

[20] K. Heyde, P. Van Isacker, M. Waroquier, J.L. Wood, and R.A. Meyer, Phys. Rep. **102**, 291 (1983).

[21] G.L. Poli et al., Phys. Rev. C **59**, R2979 (1999).

[22] K.S. Toth et al., Phys. Rev. C **58**, 1310 (1998).

[23] K. Heyde, J. Ryckebusch, M. Waroquier, and J.L. Wood, Nucl. Phys. **A484**, 275 (1988).

[24] W.F. Mueller et al., Phys. Rev. C **59**, 2009 (1999).

[25] W. Reviol et al., Phys. Rev. C **49**, R587 (1994).

[26] H. Kettunen et al., in Experimental Nuclear Physics in Europe, edited by Berta Rubio, Manuel Lozano, and William Gilletly, AIP Conf. Proc. No. 495, (AIP, Melville, NY, 1999), p. 125.

[27] J. Wauters et al., Phys. Rev. C **55**, 1192 (1997).

[28] A.J. Larabee et al., Phys. Lett. **169B**, 21 (1986).

[29] R.B. Firestone et al., Table of Isotopes, 8th ed., Vol. II (J. Wiley, New York, 1996).

[30] M. Muikku, Ph.D. thesis, Department of Physics, University of Jyväskylä, Research report No. 7/2000, and references therein.